

## ABSTRACT

### AN IoT-BASED MULTI-GAS SENSOR TO IDENTIFY FLAMEOUT PRECURSORS

Robert Ian<sup>1\*</sup>, Lok-kun Tsui<sup>2</sup>, Sleight Halley<sup>1</sup>, James Smith<sup>1</sup>, Ramiro Jordan<sup>3</sup>, Fernando Garzon<sup>2</sup>, Kamil Agi<sup>1</sup>

1. SensorComm Technologies, Inc. Albuquerque, NM.

2. Center for Micro-Engineered Materials, University of New Mexico, Albuquerque, NM.

3. Electrical & Computer Engineering, University of New Mexico, Albuquerque, NM.

\*Presenting / Corresponding Author: Robert Ian ([rian@sensorcommtech.com](mailto:rian@sensorcommtech.com))

The results have shown the existence of, and our ability to measure, precursors that can predict flameout conditions [before the flameout event] using a mixed-potential electrochemical system coupled with an IoT platform. Methane is a potent greenhouse gas with a global warming potential of 28 times that of CO<sub>2</sub> over a 100-year time span. A recent aerial sampling survey carried out in oil and gas producing regions of the US estimated that the methane destruction efficiency from flaring was 5 times higher than previously estimated. The causes of excess methane emissions from flaring operations included low efficiency burning or unlit flares. In light of the increasing concern of methane emissions to climate change, there is a need to develop sensor technology that can provide continuous monitoring, coupled with an early-warning system for flaring infrastructure to detect low methane destruction efficiency or flameout conditions. Solid state mixed potential sensors are an electrochemical sensor technology which are low-cost, robust when exposed to combustion exhaust gases, and are field-deployable. We have recently completed field tests showing that a four-electrode mixed potential sensor coupled with an IoT platform that can remotely detect the emissions of natural gas from a simulated buried pipeline. Customer discovery has identified IoT connectivity (especially through the cellular network) as an adoption barrier for the oil & gas industry due to privacy and cybersecurity concerns. Integration of ethernet ports has enabled a viable approach to data transmission, onsite data storage, and control. Alternative secure wireless strategies are currently being investigated (e.g., SCADA/satellite) that include a pathway to quantum encryption. In this work, emissions from a bench-scale methane flare were sampled by a multi-electrode mixed potential sensor. The gas feed was diluted with an increasing concentration of CO<sub>2</sub> to simulate depletion of fuel in the flare input. We observed an increase in CO detected on an Au vs. Pt electrode pair 5 minutes prior to an observed flameout (Figure 1). A complete early-warning system can be developed that autonomously monitors the gases in the flame and can predict when the system will approach a flameout condition due to interference in the gas stream.

## AFRC 2024 SYMPOSIUM PAPER

### AN IoT-BASED MULTI-GAS SENSOR TO IDENTIFY FLAMEOUT EVENTS

#### I. INTRODUCTION

Global methane emissions have increased over the past two decades [1]. Methane comes from multiple sources, both natural and man-made and is an important contributor to global warming and can be up to 84x more environmentally potent than CO<sub>2</sub> [2]. The oil & gas industry is the largest source of methane emissions in the US, responsible for approximately 30% of total emissions. Refineries use flaring as a means of reducing the amount of methane that escapes into the air from the refining process and is most of the time underestimated [3]. Industry and regulators assume 98% combustion efficiencies, but in reality, it may be closer to 91%. Optimized combustion efficiencies, managed flow rates, and even deploying alternatives to flaring (flaring wastes approximately 8% of the global natural gas production) are all levers that can be adjusted to avoid flameouts. However, flameouts do occur regularly, as much as 3-5% of the time [4]. In Texas, smoking flares (inefficient combustion) also occur on a regular basis and have logged times as long as 30 min with no appreciable response [5]. The key to mitigating flameout effects is creating an early-warning system [6]. The idea is to understand what gases are released just prior to a flameout and whether we can predict a flameout before it occurs. We refer to these “flameout fingerprints” as *precursors*. For first approximation, once a flameout occurs, there will be an increase in methane gas. The key is to understand and measure what happens just prior to the flameout. For example, is the flameout caused by a suboptimal air to fuel ratio or addition of diluent gases such as CO<sub>2</sub>? This early-warning system must include continuous monitoring, multi-gas sensors, edge and cloud analytics, and a strategy to differentiate the sources that may cause a flameout.

#### Multi-Element MPE Sensors.

- MPES devices rely on a difference in catalytic activity to generate a voltage upon exposure to test gases.
- Selectivity can be tuned by material selection, geometry, applied current bias.
- Low-cost, robust, and well suited for mass-fabrication.
- Combined with ceramic additive manufacturing to enable rapid prototyping of materials for sensitivity.
- Sensor Composition:
  - Indium Tin Oxide (ITO): CH<sub>4</sub>
  - La<sub>0.87</sub>Sr<sub>0.13</sub>CrO<sub>3</sub> (LSC): C > 1 Hydrocarbons
  - Au: NH<sub>3</sub>
  - Substrate: YSZ
  - Electrolyte: Porous YSZ

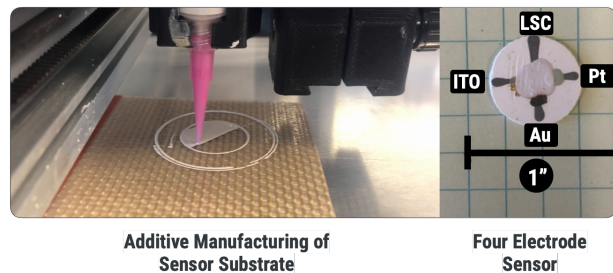


**Figure 1.** Mixed potential electrochemical sensor used in the experiments.

This program uses mixed potential electrochemical sensors to identify flameout fingerprints. Mixed potential sensors are solid-state ceramic devices with multiple dissimilar electrodes. The difference in catalytic activity on the electrodes upon exposure to both oxidizable (CH<sub>4</sub>) and reducible gases results in a mixed potential difference across the electrodes that can be measured and used as a sensing parameter [7]. The selectivity to a particular gas can be tuned by material selection, geometry, operating temperature, and applied bias. The mixed potential sensors we have developed consists of 4-electrodes as illustrated in in Figure 1 and the selection of electrode

materials were originally designed for methane emissions detection [8]. The Platinum (Pt) electrode serves as the reference. The indium tin oxide (ITO) electrode is sensitive to CH<sub>4</sub>, the La<sub>0.87</sub>Sr<sub>0.13</sub>CrO<sub>3</sub> (LSC) electrode is sensitive to heavy hydrocarbons and NO<sub>x</sub> under current bias, and the Au electrode is sensitive towards CO, NH<sub>3</sub> and H<sub>2</sub> [9]. The goal is to use a multi-gas sensor platform to determine conditions where there is inefficient flaring and/or conditions where the inefficiencies can lead to flameout conditions. For this application, we are primarily interested in using the ITO vs. Pt and Au vs. Pt signals to correlate CH<sub>4</sub> and CO as flameout precursors. Sensors were additively manufactured by robocasting of the ceramics and direct ink write for the electrodes. The sensors were then integrated with SensorComm Technologies' Internet of Things (IoT) platform which handles data acquisition and wireless transmission to the cloud. Two main technical challenges were originally proposed. The first is whether precursors exist and how can we identify them? Second, do they occur prior to a flameout event so that an early-warning system can be developed by identifying the precursors?

## II. EXPERIMENTAL SECTION

### Sensor Fabrication.

Solid-state mixed potential sensors were manufactured using direct ink write for the electrodes (Pt, ITO, LSC, and Au) electrodes following the procedures described in Halley et al. 2022 [10]. Briefly, magnesia stabilized zirconia (MSZ) substrates were prepared by robocasting of an aqueous paste, partially sintered, and the Pt conductor leads and electrode were added before sintering to full density. Next, ITO, LSC, and Au electrodes were added in sequence and sintered, followed by a porous YSZ. The sensor was then bonded with a ceramic adhesive (Aremco Ceramabond) to an Induc ceramic wire wound heater. The sensor was then inserted into a 1" Swagelok T-fitting.

### IoT Capability.

The readout electronics for the sensors includes the ability to measure multiple channels of low-level signals (down to 1mV). It also performs temperature control for the sensors and supplies power to all parts of the sensor system. The sensor connects to our IoT server over Wi-Fi or an optional 4G modem. The system stores data on both the server and on-board the sensor system as part of a data surety strategy [11]. Customer discovery has identified IoT connectivity (especially through the cellular network) as an adoption barrier for the oil & gas industry due to privacy and cybersecurity concerns. Integration of ethernet ports has enabled a viable approach to data transmission, onsite data storage, and control. Alternative secure wireless strategies are currently being investigated (e.g. SCADA/satellite) that include a pathway to quantum encryption. Feedback has also included requests for testing system capabilities (e.g., pilot programs), in addition to the underlying multi-gas sensor platform for other project initiatives.

### Sensor Testing.

Sensors were tested with controlled concentrations of gases supplied by an Environics 2000 gas mixer and the sensor voltages between the ITO, LSC, and Au electrodes were measured against the Pt electrode using a SensorComm Technologies IoT readout board. For tests where gases were drawn from an ambient atmosphere, a Parker Hannifin air pump at 0.5 SLPM was used as a

sampling pump. The sensor was heated to 532C using an external 10V power supply connected to the heater resulting in a power of 10W.

### Flameout Testing.

A bench-scale flameout test was constructed using a Bunsen burner and mass flow controllers in a fume hood. 100% CH<sub>4</sub> was supplied to the burner and diluted with Ar and CO<sub>2</sub>. A ~1 m stainless steel sampling line was placed about 2 cm above the flame and connected to the sampling pump. The stainless steel acted to dissipate the heat of the exhaust gases to prevent melting of the polymer tubing used in the sensor package.



**Figure 2.** Thermal imaging showing the Bunsen burner flame operating in the fume hood. The horizontal stainless-steel tube above the thermal imager is the sampling line.

## III. RESULTS AND DISCUSSION

### Controlled Measurement.

The sensor response to CH<sub>4</sub> and CO were measured separately followed by a mixture of the two gases. The sensor was exposed to a test gas mixture containing 21% O<sub>2</sub> and balanced with N<sub>2</sub> at a flow rate of 150 CCM. The CH<sub>4</sub> concentration was varied from 100-5000 ppm and the CO concentration was varied from 25-350 ppm. The binary mixture consisted of 50-300 ppm CO and 60-600 ppm CH<sub>4</sub>. The sensor response is shown in Figure 3 for the single-gas measurements and Figure 4 for the binary mixtures. CH<sub>4</sub> results in a weak signal in the Au vs. Pt pair and a strong signal in the ITO vs. Pt pair. CO results in a strong signal from both ITO vs. Pt and Au vs. Pt. The mixture (Figure 4) shows the sensor response biased towards CO sensitivity. The test was conducted with 100% CH<sub>4</sub> instead of a natural gas mixture, and the increased sensitivity of C<sub>2</sub>H<sub>6</sub> may result in better separation between these two gases. Other approaches to improve the potential for quantification include operation of multiple sensors at different temperatures as CH<sub>4</sub> would be easier to detect at higher temperature due to its lower reactivity compared with CO.

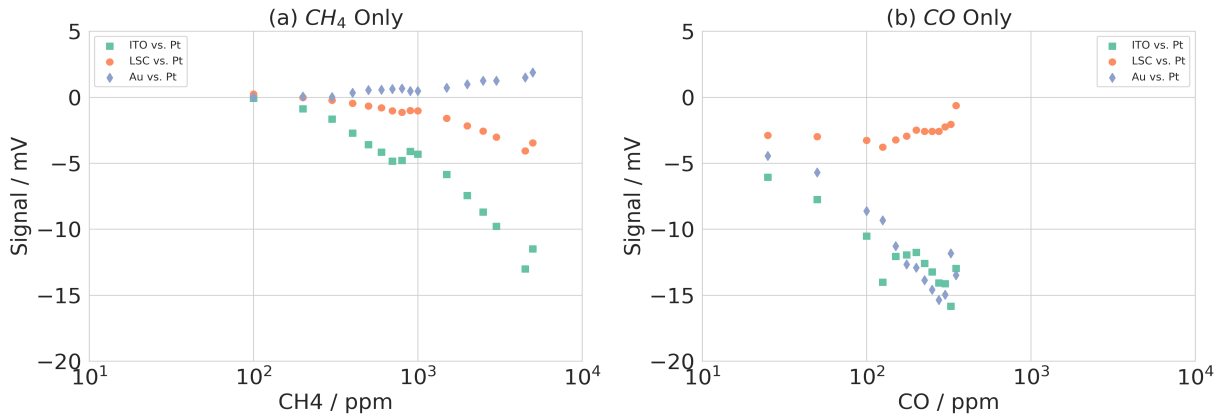


**Figure 3.** Comparison of the sensor response of CH<sub>4</sub> and CO. CH<sub>4</sub> induces a strong response in the ITO vs. Pt pair only while CO induces a response in both ITO vs. Pt and Au vs. Pt.

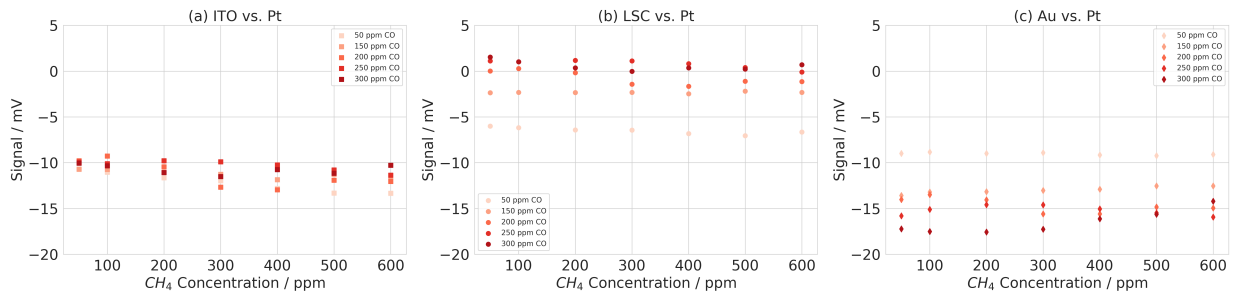


**Figure 4.** Sensor response of mixtures of CO and CH<sub>4</sub> indicate that CO is the dominant gas, and no correlation is observed between the concentration of CH<sub>4</sub> and the signals measured.

## Simulated Flameout.

We simulated a flameout event to see if the system was capable of identifying (with early-warning) a flameout condition. A time vs. signal plot appears in Figure 5. In this test, the fuel stream of 100% CH<sub>4</sub> was diluted with CO<sub>2</sub> to reduce the ratio of CH<sub>4</sub> to CO<sub>2</sub> until a flameout occurs. While a real natural gas mixture is ideal for testing, we were unable to procure a flammable mixture before the end of the project period. Because of the relative inertness of CO<sub>2</sub> to our sensors, this species is not detected. The fuel was supplied to the burner at a constant flow rate of 200 CCM. Air was supplied by the vents on the base of the Bunsen burner and not directly controlled. At a CH<sub>4</sub>:CO ratio of 1:1, an increase in the Au vs. Pt signal to 10 mV is observed, indicating a CO concentration of approximately 100 ppm. In this transition period, the high concentration of CO<sub>2</sub> pushes the combustion reaction equilibrium towards incomplete combustion with CO as a product. The flame was visually observed to go out at the timestamp of 1700 and an increased signal of ITO and LSC vs. Pt is seen with the Au vs. Pt signal dropping to near zero. This indicates that the sensor is detecting unburned CH<sub>4</sub>, which is what we expect from an unlit flame. This experiment

illustrates that it is possible to detect a chemical fingerprint of a flameout event from this cause, fuel dilution, with a lead time of approximately 5 minutes. Other potential causes involving oxidizer starvation and dilution with other gas species such as  $N_2$  would have different chemical fingerprints such as excess hydrocarbon or  $NO_x$ . An early-warning system that can take the chemical fingerprints and categorize them by cause would be able to direct the operator what actions need to be taken to address the issue.



**Figure 5.** The simulated flameout condition was reported near 17:00. The Au vs. Pt has the most prominent early-warning and provides approximately 5 min autonomous early-warning.

The early-warning system is predicated on anomalies in the data. Because the system collects and analyzes time-series data, individual measurements are not as important as system trends and/or behaviors over time. Results become more accurate the longer the system operates. Analytics identify data anomalies with each of SensorComms' current IoT platforms. The effectiveness of the early-warning system is governed by the sensitivity of the sensor. In general, enhanced sensitivity of the sensor yields more robust anomaly detection.

### Characterization of the Flame – Mass Spectrometer.

A mass spectrometer was used to characterize the Bunsen burner flame to see if there are other gases that could be measured. The sampling line was connected to an MKS Cirrus 2 mass spectrometer and the results are shown in Figure 6 and Figure 7. Figure 6 measures the sampled  $CO_2$  and  $CH_4$  as the interference gas ( $CO_2$ ) is increased. When the burner is lit, the  $CH_4$  goes to zero while the  $CO_2$  concentration increases. The measured  $CO_2$  signal also increases as the fuel is



diluted with additional CO<sub>2</sub>. One possible reaction that we wanted to eliminate was dry reforming which would produce H<sub>2</sub> and heavy hydrocarbons as a byproduct. MS detected no appreciable hydrogen or heavy hydrocarbons (Figure 7). There is a slight increase in the CO-N<sub>2</sub> signal when the CH<sub>4</sub> was first lit. These two molecules are grouped together since they have identical molecular mass. Previous work has shown that Au vs. Pt is sensitive to both CO and H<sub>2</sub>, but since no H<sub>2</sub> was detected, we can attribute the sensor signal to CO. A complimentary technique we will explore in the future is gas phase FTIR analysis which will more easily discriminate between identical mass species like CO and N<sub>2</sub>.

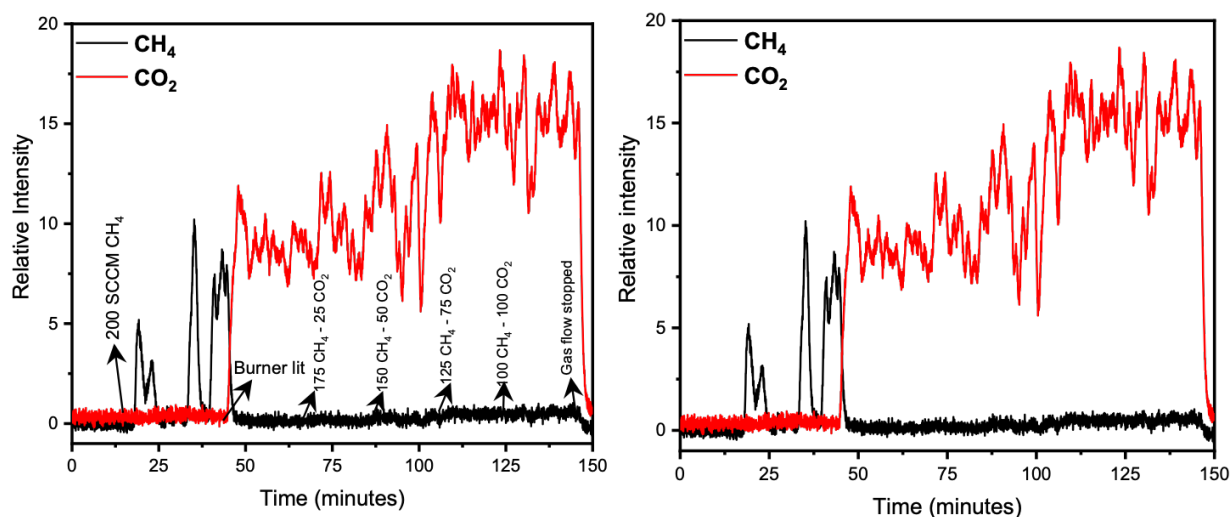


**Figure 6.** Mass spectrometer characterization of the flame. The left figure shows the individual events, the right figure is the actual trace.

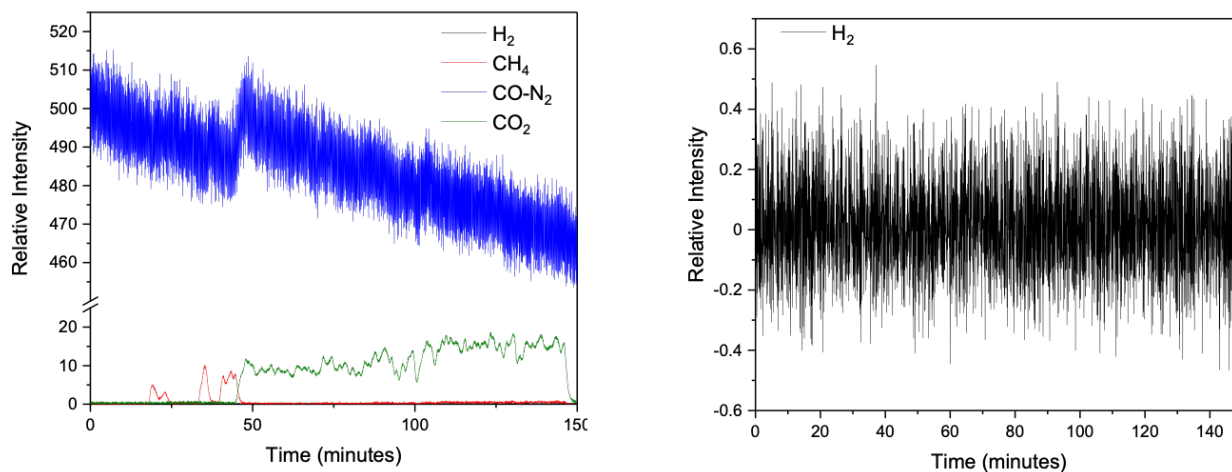


**Figure 7.** The left image shows the measurement of CO-N<sub>2</sub> (mass 28). A small increase in CO is shown when the CH<sub>4</sub> is first lit. The right image is measuring H<sub>2</sub>. Note no appreciable hydrogen signature thus likely no heavy hydrocarbons produced.

## Improving Sensor Performance – Sensitivity

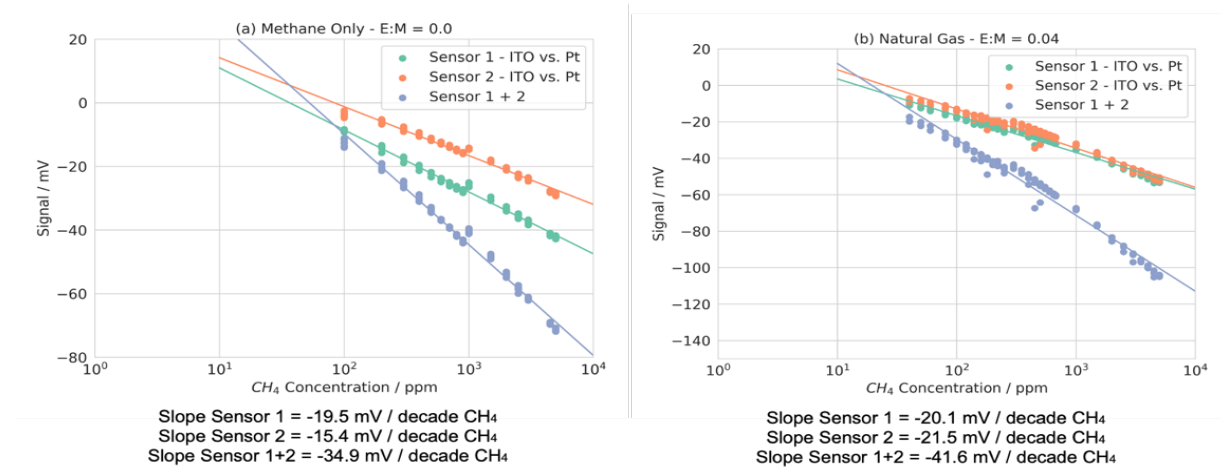


**Figure 8.** Results of two sensors connected in series. The system provides lower signal detection capability and more resolution for high dynamic range signals.

The results of placing two sensors in series are shown in Figure 8 to investigate a method to increase sensitivity. The blue curve is the sum signal. As expected, the voltages from the individual signals add and so the system remains linear. Thus, sensitivity (measured in mV/decade) in the large signal range shown in the figure exhibit a log-linear behavior which approximately doubles when the sensors are placed in series. This implies that at lower signal levels (lower concentrations), the two-sensor system will be able to measure lower levels of methane. This also relaxes the analog voltage sensitivity requirements on the IoT hardware. We expect that sensors in series not only provide a lower limit of detection, but also more resolution when looking at high dynamic range signals.

## Early-Warning System

Figure 9 shows cross-plots of normalized voltage readings from different sensors in the simulated flameout experiments. With  $R^2$  values of 0.66 and 0.25 respectively, we observe different degrees of correlation between the variables. The plot with an  $R^2$  of 0.66 indicates a moderate to strong correlation between ITO vs Pt. & LSC vs Pt. voltage readings. However, the existence of unexplained variance highlights that each variable still carries unique information. On the other hand, the plot with an  $R^2$  of 0.25 shows a much weaker correlation between ITO vs. Pt & Au vs. Pt voltage readings. This low correlation further emphasizes that each sensor measurement contributes distinct and relevant information. Therefore, despite some level of correlation, these plots collectively illustrate that the variables are not perfectly correlated, reinforcing the value of each measurement.



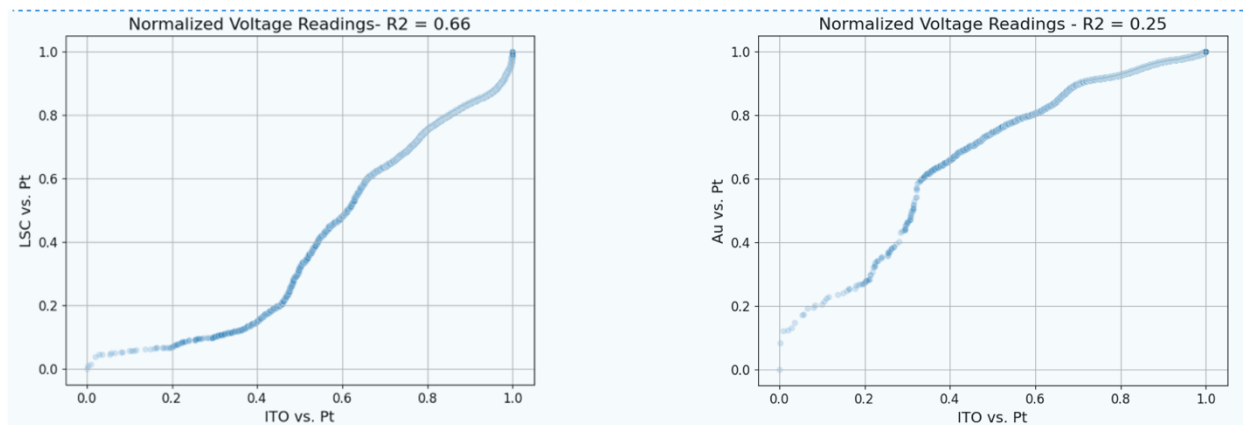


**Figure 9.** Normalized voltages of each individual sensor. Combining responses improves accuracy of identification and quantification.

In the conducted simulation of a flameout scenario, distinct precursors are evident, particularly when examining the signals from Au versus Pt and ITO versus Pt. These precursors indicate that such signals could be instrumental in developing a model capable of predicting flameouts, thereby substantially mitigating methane emissions. Considering the sparse incidence of such events in this experimental phase, a Z Scoring algorithm (Figure 10) has been employed to discern anomalies preceding a flameout, highlighting its potential for early detection and prevention.

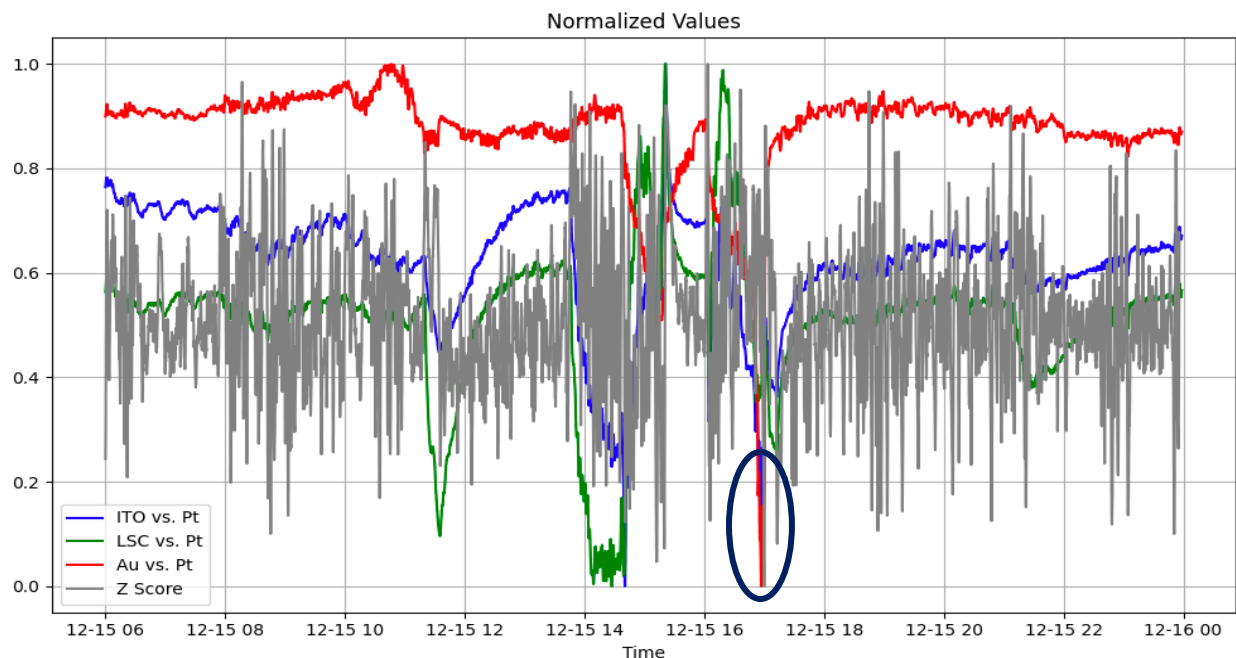


**Figure 10.** Simulated flameout using Bunsen burner from Figure 2. Anomaly detection using thresholding and Z-score. Note flameout happened at approximately 12-15 17:00 highlighted by the oval.

## Conclusions

There were 5 goals that were completed in this program:

1. Can a fundamental emission signature can be identified?
2. What are the minimum thresholds required to sense precursors?
3. What are the gases in the IoT-based sensor platform needed?
4. Can this approach provide an early-warning system?
5. Can we improve sensitivities of individual sensor components?

In this work, we have determined that a CO<sub>2</sub> dilution of the fuel results in an increase in CO 5 min prior to a flameout event. For the flow rates in the simulations, this corresponds to approximately 100 ppm CO, so we think a detection range of 10-1000 ppm CO would be able to detect this condition. Finally, we have demonstrated the increased sensitivity in terms of mV/decade gas concentration by putting two sensors in series.

Customer discovery identified IoT connectivity (through the cellular network) as an adoption barrier for the oil & gas industry due to privacy and cybersecurity concerns. Integration of ethernet ports has enabled a viable approach to data transmission, onsite data storage, and control. Feedback has also included requests for testing system capabilities (e.g., pilot programs), in addition to the underlying multi-gas sensor platform for other project initiatives.

## Acknowledgments

This work was sponsored by DOE SBIR Office of Science Award DE-SC0023770 and Office of Fossil Energy and Carbon Management Award FE0031864.

## REFERENCES

1. Global methane levels soar to record high, Q. Schiermeier, 14 July 2020, <https://www.nature.com/articles/d41586-020-02116-8>
2. Climate Change Connection, CO<sub>2</sub> Equivalents, <https://climatechangeconnection.org/emissions/co2-equivalents/>
3. Flaring allows more methane into the atmosphere than we thought, J. Lynch, College of Engineering, 29 September 2022, <https://news.umich.edu/flaring-allows-more-methane-into-the-atmosphere-than-we-thought/>
4. Flaring and Venting Research & Development Activities, Report to Congress, August 2021, <https://www.energy.gov/sites/default/files/2021-08/Flaring%20and%20Venting%20Report%20to%20Congress%20Report.pdf>
5. Texas Doesn't Care About Smoking Flares. They Should., Earthworks Blog, J. McDonald, 20 July 2022, <https://earthworks.org/blog/texas-doesnt-care-about-smoking-flares-they-should/>
6. Detecting Fugitive Methane Leaks for Public Safety, Eos, K. Brown, 14 January 2019, <https://eos.org/articles/detecting-fugitive-methane-leaks-for-public-safety>
7. A review of zirconia oxygen, NO<sub>x</sub>, and mixed potential gas sensors – History and current trends, ScienceDirect, S. Halley, 1 November 2022, <https://doi.org/10.1016/j.snb.2022.132363>; A review of mixed-potential type zirconia-based gas sensors, Springer Link, N. Miura, 28 May 2014, <https://link.springer.com/article/10.1007/s11581-014-1140-1>; Solid-state mixed potential gas sensors:

- theory, experiments and challenges, ScienceDirect, F. Garzon, 2 November 2000, [https://doi.org/10.1016/S0167-2738\(00\)00348-9](https://doi.org/10.1016/S0167-2738(00)00348-9)
8. Field Testing of a Mixed Potential IoT Sensor Platform for Methane Quantification, ECS Sensors Plus, S. Halley, et al, 9 February 2024, <https://iopscience.iop.org/article/10.1149/2754-2726/ad23df>; Massive enhancement in sensitivity of mixed potential sensors towards methane and natural gas through magnesia stabilized zirconia low ionic conductivity substrate, Sensors and Actuators. B, Chemical, S. Halley, et al, 1 October 2023, <https://doi.org/10.1016/j.snb.2023.134031>; Combined Mixed Potential Electrochemical Sensors and Artificial Neural Networks for the Quantification and Identification of Methane in Natural Gas Emissions Monitoring, Journal of The Electrochemical Society, S. Halley, et al, 16 September 2021, <https://iopscience.iop.org/article/10.1149/1945-7111/ac2465>
  9. Development and testing of an electrochemical methane sensor, Sensors and Actuators B: Chemical, K. Sekhar, et al, 2 June 2016, <https://doi.org/10.1016/j.snb.2015.12.100>; Automatic signal decoding and sensor stability of a 3-electrode mixed-potential sensor for NO<sub>x</sub>/NH<sub>3</sub> quantification, Electrochimica Acta, L-K. Tsui, et al, 1 September 2018, <https://doi.org/10.1016/j.electacta.2018.06.133>; Quantitative decoding of the response a ceramic mixed potential sensor array for engine emissions control and diagnostics, Sensors and Actuators B: Chemical, L-K. Tsui, et al, October 2017, <https://doi.org/10.1016/j.snb.2017.04.060>; A Three Electrode Mixed Potential Sensor for Gas Detection and Discrimination, ECS Transactions, Vol 75 No 16, 2016, L-K. Tsui, et al, <https://iopscience.iop.org/article/10.1149/07516.0009ecst>
  10. Massive enhancement in sensitivity of mixed potential sensors towards methane and natural gas through magnesia stabilized zirconia low ionic conductivity substrate, Sensors and Actuators B: Chemical, 1 October 2023, S. Halley, et al, <https://doi.org/10.1016/j.snb.2023.134031>
  11. SensorComm Technologies, Inc., <https://sensorcommtech.com>